Sorting and trafficking of proteins in oligodendrocytes during myelin membrane biogenesis

Klunder, Lammert

Chapter 2

Sorting signals and regulation of cognate basolateral trafficking in myelin biogenesis

Bert Klunder, Wia Baron, Cobi Schrage, Jenny de Jonge, Hans de Vries and Dick Hoekstra

Accepted for publication in Journal of Neuroscience Research

Abstract

A detailed understanding of trafficking pathways in mature oligodendrocytes (OLGs) is essential for addressing issues aimed at controlling (re)myelination by modulating myelin-directed transport. Previously, we have shown that the viral marker proteins, HA and VSV G, reaching in polarized epithelial cells the apical and basolateral surface, respectively, are primarily transported to plasma membrane and myelin sheet, respectively, in OLGs. Here, we demonstrate that in OLGs similar basolateral sorting signals as in epithelial cells may target proteins to the myelin sheet, emphasizing the basolateral- and apical-like nature of myelin sheet and plasma membrane, respectively. Thus, substitution of essential amino acids reverses the direction of targeting of these proteins, whereas elimination of apical targeting of HA coincides with its dissipation from detergent-resistant microdomains. Furthermore, protein kinase C (PKC) activation negatively regulated transport of the OLG resident transmembrane protein PLP to the myelin sheet, like that of VSV G as shown previously, but did not affect the localization of the membrane-associated myelin specific proteins MBP and CNP. These data imply that several, distinctly regulated pathways operate in myelin sheet directed transport, which at least partly rely on a cognate basolateral sorting signal.

Introduction

During development, oligodendrocytes (OLGs), the myelinating cells of the central nervous system (CNS), express large quantities of myelin proteins and lipids that are transported from the cell body to the processes, which form myelin sheaths that enwrap axons to facilitate nerve impulse signal conduction. *In vitro*, OLGs grown in mono-culture follow the same developmental pattern as *in vivo*, i.e., all the myelin components are expressed in a coordinated fashion and transported to the different subdomains in the myelin sheet (Pfeiffer *et al.*, 1993; Gielen *et al.*, 2006), corresponding to non-compacted myelin-like membranes. Given the high glycosphingolipid content of the myelin sheet as compared to the plasma membrane of OLGs, it is tempting to correlate the membrane organisation of the myelin sheet to that of the apical domain of polarized epithelial cells (Weimbs *et al.*, 1997; Lafont *et al.*, 1999; de Vries and Hoekstra, 2000; Gielen *et al.*, 2006). Intriguingly, we observed that the biogenesis of the myelin sheet *in vitro* involves basolateral-like features, rather than features typical of apical membrane directed transport, seen in polarized epithelial cells (de Vries *et al.*, 1998). Thus in OLGs the apical domain marker influenza hemagglutinin (HA) is typically transported to the cell body plasma membrane, and localizes to detergent resistant microdomains, whereas the basolateral membrane marker vesicular stomatitis virus glycoprotein (VSV G) accumulates in the myelin sheet, and is solubilized upon detergent treatment of the cells. By extrapolation, this would imply that in OLGs a cognate basolateral rather than an apical pathway is used to transport proteins to the myelin sheet.

The operational definitions concerning polarity and polarized trafficking have been largely defined based upon work in Madin-Darby canine kidney (MDCK) cells. In these cells polarity is generated by sorting of apical- and basolateral-directed proteins in the *trans*-Golgi network (TGN) and/or endosomes (Ikonen and Simons, 1998; Matter, 2000; Gravotta *et al.*, 2007). Basolateral sorting signals are mainly restricted to the cytosolic tails of proteins, which frequently contain crucial tyrosine- or di-leucine-based amino acid motifs. It has been shown that the presence of a tyrosine at position 501 in the C-terminal part of VSV G is an important intramolecular signal for basolateral sorting (Brewer and Roth, 1991; Hunziker *et al.*, 1991; Muth *et al.*, 2003). Furthermore, by converting cysteine 543 to tyrosine in the cytoplasmic domain of HA, the protein is no longer sorted apically but acquires both a basolateral sorting signal and an internalization signal (Brewer and Roth, 1991; Lazarovits and Roth, 1988; Lin *et al.*, 1997). Examples of apical delivery signals or

sorting mechanisms often rely on lipid-lipid or lipid-protein interactions and partitioning in membrane microdomains (Ikonen and Simons, 1998; Matter, 2000; Delacour and Jacob, 2006).

Apart from 'intrinsic' signals, protein kinase activity has been recognized as an important regulator of polarized trafficking in MDCK (Pimplikar and Simons, 1994; Cardone *et al.*, 1994) and polarized HepG2 liver cells (Zegers and Hoekstra, 1997; Tyteca *et al.*, 2005). Such knowledge is lacking in mature OLGs, but in OLG progenitors PKC activation impedes the sheet-directed 'basolateral-like' pathway (VSV G), and activates 'apical-like' (HA) trafficking to the membrane of the cell body (Baron *et al.*, 1999).

We therefore further examined the polarized nature of mature OLGs, in particular the relevance of basolateral-like trafficking to the sheet. Here, we show that the basolateral tyrosine 'signal' in the C-terminal part of viral model proteins is sufficient (HA) and essential (VSV G) for myelin sheet targeting, while transport of specific myelin proteins to the sheet is differentially affected upon PKC activation. Our results corroborate that myelin-directed trafficking is served by a cognate basolateral transport pathway, and regulated by distinct signalling pathways.

Materials and Methods

Materials

Dulbecco's Modified Eagle's Medium (DMEM, with 4500 mg/l Glucose and L-glutamine), L-glutamine, penicillin/streptomycin and Geneticin (G418) were purchased from Gibco Invitrogen Corporation (Paisley, UK). Fetal calf serum (FCS) was obtained from Bodinco (Alkmaar, The Netherlands). The transfectant FuGene 6 and protease inhibitor cocktail tablets (Complete Mini) were obtained from Roche Diagnostic Corp (Mannheim, Germany). Growth factors FGF-2 and PDGF-AA were supplied by PeproTech Inc. (London, UK). Paraformaldehyde was supplied by Merck (Darmstadt, Germany). Nonidet P40 (NP40) was purchased from Fluka BioChemica (Buchs, Switzerland). Phorbol-12-myristate-13 acetate (PMA) and bisindolylmaleimide I (BIM) were from Calbiochem-Novabiochem Corporation (La Jolla, Ca). Sulfo-NHS-LC-Biotin was obtained from Pierce (Rockford, IL). Streptavidin was obtained from Upstate Lake Placid (New York, NY). All other chemicals were purchased from Sigma Chemical Co. (St. Louis. MO).

Antibodies

The monoclonal antibody against PLP (Greenfield *et al.*, 2006) and the polyclonal antibody against HA were generously provided by Prof. Dr. V. Kuchroo (Center of Neurological Diseases, Harvard Medical School, Boston, MA) and Prof. Dr. I. Braakman (Research Group of Cellular Protein Chemistry, Utrecht, the Netherlands), respectively. The R-mAb hybridoma (Ranscht *et al.*, 1982) was a kind gift of Dr. Guus Wolswijk (NIBR, Amsterdam, The Netherlands). The monoclonal antibodies anti-VSV G (IgG1) and anti-CNPase (IgG1) were obtained from Sigma (St. Louis, MO). Anti-MBP was purchased from Serotec (Oxford, UK). Fluorescein isothiocyanate (FITC) and tetramethylrhodamine isothiocyanate (TRITC) conjugated antibodies were supplied by Jackson ImmunoResearch Laboratories, Inc. (West Grove, PA). Secondary horseradish peroxidase (HRP)-conjugated antibodies were obtained from Amersham Biosciences (Little Chalfort, UK).

Constructs

General procedures for cloning and DNA manipulations were performed as described by Sambrook *et al.* (1989). The cDNA's encoding HA, HAY$^+$, VSV G and VSV GY$^-$ were a kind gift of Dr. M.G. Roth (Department of Molecular Medicine, Cleveland, OH). For cloning the viral genes in the retroviral vector pLXIN (Clontech Biosciences, Mountain View, CA), an XhoI restriction site in close distance of the ATG start codon of the HA, HAY$^+$, VSV G, VSV GY$^-$ genes and an XhoI restriction site after the stop codon were introduced by the polymerase chain reaction. The following primers were used:

5' GGTACACGCTTCTCGAGAAGCTTATGTAC 3' (forward HA, HAY$^+$),

5' GCACCCGGGATCCTCGAGAACTAGTGGATC 3' (reverse HA, HAY$^+$),

5' CGATCTTTTTCCTCGAGACTATGAAGTG 3' (forward VSV G, VSV GY$^-$)

5' CAGGGATGCACTCGAGATCCTCTAG 3' (reverse VSV G, VSV GY$^-$)

The PCR products were digested with restriction enzyme Xho1 (Gibco Invitrogen Cooperation, Paisly, UK) and ligated with the 1.8 kb retroviral vector pLXIN. Recombinant plasmids were grown in Escherichia coli DH5α cells, and plasmids with the cDNA insert in the correct orientation with respect to transcription were identified by restriction analysis. The orientation and the integrity of the obtained pLXIN constructs were confirmed by DNA sequencing.

Production of retroviral particles

The production of retroviral particles and the subsequent infection of OLG progenitors were performed according to Relvas *et al.* (2001). Briefly, for production of recombination-deficient retroviruses, the constructs were transfected into the GP+E86-packaging cell line (Genetix Pharmaceuticals Inc., Cambridge, MA), using the FuGene 6 transfection reagent. Two days after transfection, cells were collected, diluted 5-fold and cultured under selection in packaging cells medium (DMEM medium containing 10% FCS) supplemented with 1 mg/ml G418 (corrected for inactivity) until resistant clones appeared (70% confluent). The cells were subsequently washed with PBS, and packaging cells medium without G418 was added. The conditioned medium was collected after 24 hrs, filtered (Schleicher and Schuell, Dassel, Germany, 0.45 μm pore size), and either used immediately or stored frozen at -80 °C.

Cell culture

Primary OLG cultures were prepared from brains of 1-2 day old Wistar rats as described previously (Baron *et al.*, 1998), with slight modifications. Briefly, after decapitating the rats, the forebrains were removed and the cells were dissociated, first mechanically and then with papaine (30 U/ml) in the presence of L-cysteine (0.24 mg/ml) and DNase (10 μg/ml) for 1 hr at 37°C. A single cell suspension was prepared by repeated pipetting in a trypsin inhibitor solution (1 mg/ml). After centrifugation, the cells were resuspended in DMEM medium, containing 10% FCS, and seeded into 75 cm^2 flasks (Nalge Nunc International, Roskilde, Denmark), at approximately 1.5 brain per flask. The flasks had been precoated with poly-L-Lysine (PLL, 5 μg/ml). The OLG progenitor cells appear as round-shaped, phase dark cells on top of monolayers of flat type-1 astrocytes. After 11-12 days in culture, the OLG progenitor cells were isolated by mechanical shaking at 240 rpm over a time interval of 18-20 hrs, as described by McCarthy and de Vellis (1980), which was followed by differential adhesion to remove astrocytes and microglia. The OLG progenitor cells were plated in proliferation SATO medium (Buttery *et al.*, 1999; Maier *et al.*, 2005), supplemented with the growth factors FGF-2 (10 ng/ml) and PDGF-AA (10 ng/ml). For biochemical assays, cells were plated at a density of 1 X 10^6 cells per 100 mm PLL-coated (5 μg/ml) dish and for immunocytochemical studies the OLG progenitors were seeded at a density of 2 X 10^4 cells per well on PLL-coated permanox chambers slides (Nunc). After two days in proliferating medium, differentiation was induced by growth factor withdrawal and

further culturing in SATO medium supplemented with 0.5% FCS. After 10 days on differentiation medium cells were left either untreated (control) or exposed to 100 nM PMA, with or without the PKC inhibitor BIM (0.5 μM) for 24 hrs after which they were analyzed as indicated.

Retroviral infection

OLG progenitor cells cultured for 48 hrs in proliferation medium (SATO containing PDGF-AA and FGF-2) were retrovirally infected with the HA, HAY$^+$, VSV G and VSV GY$^-$ constructs, prepared as described above, for 16-18 hrs in media that contained 8 μg/ml polybrene, 10 ng/ml FGF-2 and 10 ng/ml PDGF-AA. The cells were cultured for another 24 hrs in proliferation medium and then cultured under selection in proliferation medium, supplemented with 400 μg/ml G418 (corrected for inactivity) for 5 days. After selection the cells were cultured on differentiation medium (SATO supplemented with 0.5% FCS) for 9 days to obtain fully mature OLGs bearing myelin-like membranes (myelin sheets).

Viral infection of cells

VSV strain San Juan A was a kind gift from Dr. Peter Rottier (University of Utrecht). Cells were infected with virus as described previously (Braakman *et al.*, 1991; de Vries *et al.*, 1998). In brief, cells were rinsed twice with culture medium, pH 6.8, before adding the virus. Cells were infected for 1 hr at 37°C with the virus in culture medium, pH 6.8, without CO_2. Then the medium was removed, fresh culture medium (pH 7.6) was added and cells were incubated for 5.5 hrs at 37°C under an atmosphere of 5% CO_2. Viral concentrations were chosen such that almost all cells were infected. When PMA was used with virus-infected cells it was added 24 hrs before infection at a concentration of 100 nM and removed just prior to addition of the virus.

Immunocytochemistry

Paraformaldehyde (PFA)-fixed cells (4% PFA in phosphate-buffered saline (PBS) for 20 min at room temperature (RT)) were rinsed with PBS and blocked and permeabilized for 30 min with 10% FCS and 0.1% TX-100 (in PBS), respectively. For staining with R-mAb, which detects the surface-localized galactolipids GalCer and sulfatide, the permeabilization step was omitted. The cells were subsequently incubated for 1-2 hrs with diluted primary antibodies (VSV G 1:100, HA 1:50, PLP 1:10, MBP 1:25, R-mAb 1:10, and CNP 1:50) in PBS,

supplemented with 2.5% FCS and 0.1% TX-100 (incubation buffer). The cells were washed with PBS and incubated for 30 min at RT with appropriate FITC- or TRITC-conjugated secondary antibody diluted in incubation buffer. To prevent image fading, the cells were covered with 2.5% 1,4-diazobicyclo[2.2.2]octane (DABCO, Janssen Chimica, Beerse, Belgium) in 90% glycerol/ 10% PBS, after washing with PBS. The cells were analyzed with an Olympus AX70 fluorescence microscope, equiped with analySIS software. Data were processed using Paint Shop Pro and/or Adobe Photoshop software.

Preparation of detergent extracts

The cells were washed with PBS, and harvested by scraping the cells with a rubber policeman in ice-cold TNE lysis buffer (20 mM Tris HCl pH 7.4, 150 mM NaCl, 1 mM EDTA, 1% TX-100 and a cocktail of protease inhibitors). Cells were lysed for at least 30 min on ice, and the protein content was measured by a Bio-Rad D_C protein assay (Bio-Rad, Hercules, CA) using BSA as standard. From equal protein amounts, soluble and insoluble fractions were separated by centrifugation at 13.000 rpm for 15 min at 4 °C. Pellets (insoluble) and supernatants (soluble) were mixed with SDS reducing sample buffer, heated for 2 min at 95ºC or 30 min at 37°C, and subjected to SDS-PAGE and Western blotting.

Surface protein biotinylation

After washing twice with ice-cold PBS, the cells were incubated for 2 hrs with Sulfo-NHS-LC-Biotin (0.1 mg/ml in PBS) at 4°C. Excess biotin was removed by washing the cells three times 5 min with cell wash buffer (65 mM Tris-HCl, pH 7.5, 150 mM NaCl, 1 mM $CaCl_2$, 1 mM $MgCl_2$) and once with PBS. The cells were harvested in PBS by scraping with a rubber policeman, and pelleted at 7.000 rpm for 5 min at 4°C). Cell pellets were lysed in TNE lysis buffer on ice for 30 min and the protein content was measured by a Bio-Rad D_C protein assay (Bio-Rad, Hercules, CA) using BSA as standard. Equal amounts of protein were incubated with streptavidin-agarose (SA-agarose) in a head over head tumbler overnight at 4 °C. SA-agarose (biotinylated protein, i.e. surface localised) was washed 4 times with ice-cold cell wash buffer supplemented with 1% NP40 and 0.35 M NaCl, once with PBS, and heated for 2 min at 95 °C in 2x SDS reducing sample buffer. The non-bound fraction (non-biotinylated proteins, i.e. the fraction localized intracellularly) was concentrated by trichloric acid (TCA) precipitation. In brief, the fractions were adjusted to a final volume of 1 ml with TNE and treated with sodiumdeoxycholate (25 mg/ml) for 5 min at 4 °C, followed

by precipitation with 6.5% TCA for 15 min at 4 °C. Precipitates were centrifugedat 10000 rpm for 20 min at 4°C. The pellets were dried and resuspended in 2x SDS reducing sample buffer, and after the pH was adjusted to 6.8 by exposure to ammonia, the samples were heated for 2 min at 95 °C. Both the biotinylated and non-biotinylated fraction were subjected to SDS-PAGE and Western blotting.

SDS-PAGE and Western Blotting

Samples were loaded onto 10 or 12.5% SDS-polyacrylamide gels and transferred to either nitrocellulose (Bio-Rad) or PVDF membranes (Millipore) by semi-dry blotting. The membranes were blocked with 5% nonfat dry milk in Tris buffered saline (TBS) to inhibit nonspecific binding. The membranes were washed and incubated for 30 min at RT with appropriate primary antibodies (VSV G 1:1000, HA 1:1000, and PLP 1:50) in TBS with 0.5% nonfat dry milk and 0.1% Tween (TBS-TM). After washing with TBS-T, the membranes were incubated for 1 hr at RT in appropriate horseradish peroxidase-conjugated antibodies at a 1:2000 dilution in TBS-TM. The signals were visualized by ECL (Amersham, Pharmacia Biotech) and quantified by Paint Shop Pro and Scion Image Software. Statistical analysis was performed using the appropriate Student's t-test. Values are expressed as means ± standard error (SE). In all cases a p-value < 0.05 was considered significant.

Results

The localization of VSV G and HA in oligodendrocytes is determined by their targeting sequences

To define molecular requirements for apical-like and basolateral-like sorting and targeting in OLGs to plasma membrane and myelin sheet, respectively, trafficking was determined of wild-type (wt) and mutant forms of the viral marker proteins HA and VSV G. Since complete viruses with a specific mutation in their (glyco-) proteins are difficult to obtain, while primary OLGs are difficult to transfect, we made use of a retroviral expression system to express wt and mutant forms of the viral proteins. Notably, after selection, with the retroviral expression system essentially all cells of the population express the protein. For the glycoprotein VSV G, the tyrosine (Y) residue at position 501 in the cytoplasmic domain, relevant to its basolateral sorting in epithelial cells (Hunziker *et al.*, 1991; Muth and Caplan, 2003), was replaced by a serine (S) (VSV GY^{-}, Thomas and Roth, 1993). Furthermore, in the short, 12-amino acid long, cytoplasmic domain of HA a cysteine (C) at position 543 was

substituted for a tyrosine (HAY+, Brewer and Roth, 1991) (fig. 1A), as a result of which it's apical sorting in polarized MDCK cells is abrogated (Lin *et al.*, 1997).

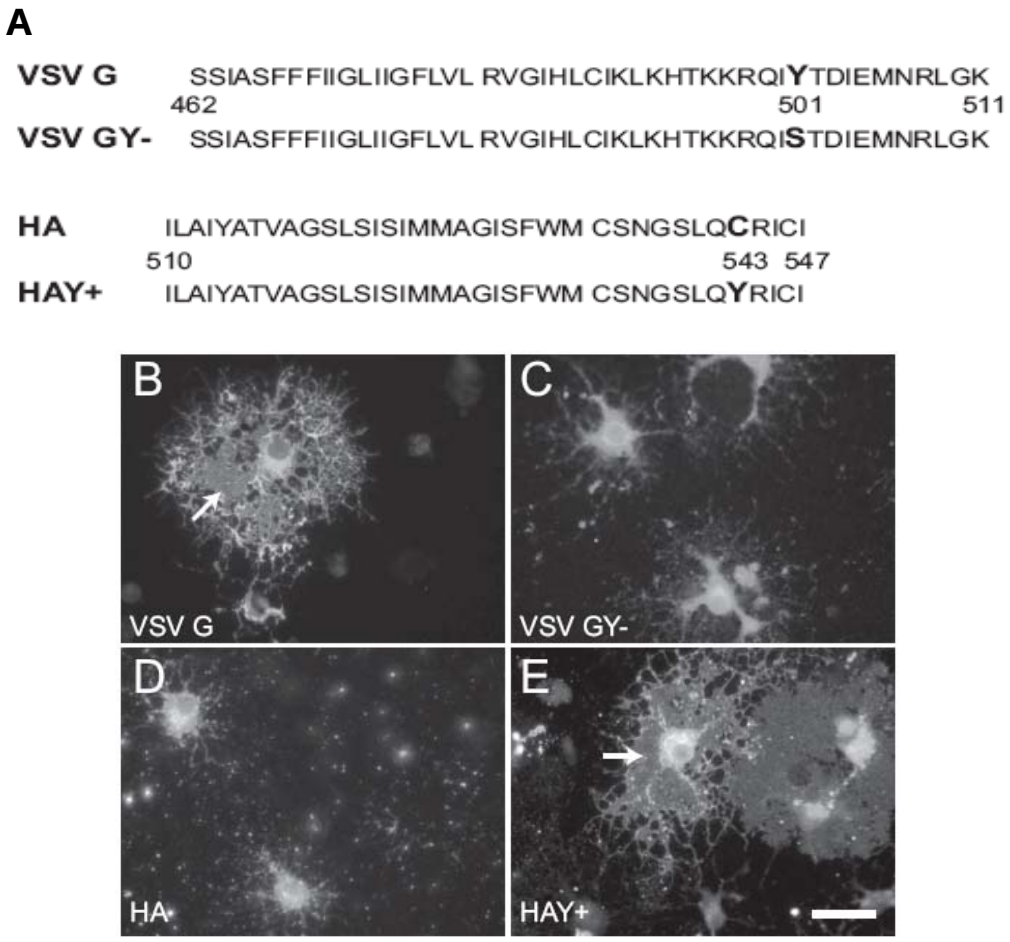

Figure 1: (A) Primary structures of the sorting domains in VSV G and HA. The amino acid sequences of the relevant parts of VSV G and influenza HA are shown. In the VSV G transport mutant VSV GY- the tyrosine (Y) residue at position 501, necessary for basolateral sorting, has been replaced by a serine. In the HA mutant HAY+, cysteine residue 543 has been replaced by a tyrosine (Y) to comply with basolateral-type trafficking requirements. (B-E). Localization of wild-type and mutant forms of the viral marker proteins HA and VSV G. OLG progenitors were retrovirally infected with wt VSV G (B), VSV GY- (C), wt HA (D) and HAY+ (E), differentiated for 9 days and the distribution of the proteins was determined by (immuno)fluorescence microscopy, as described in Materials and Methods. Representative cells out of three independent experiments are shown. Scale bar is 20 µm. Note that wt VSV G and mutant HAY+ are localized in the myelin-like membranes, i.e. the myelin sheet (arrows), whereas wt HA and mutant VSV GY- are localised to the cell body and primary processes.

The localization of the wt and mutant viral proteins in mature primary OLGs was subsequently analyzed by immunofluorescence. As shown in figure 1, apart from being expressed in the cell body and primary processes of mature OLGs, wt VSV G is also prominently present in the sheets (arrow, fig. 1B). In contrast, VSV GY- was largely localized to the cell body and primary processes, implying that the mutant protein apparently lost its

ability of acquiring access to the myelin sheet (fig. 1C). Thus, the mislocalization of VSV GY- demonstrates that the unique tyrosine in position 501 in VSV G is critically important for functioning as a basolateral-like sorting signal, instrumental in mediating transport to the myelin sheet in OLGs (de Vries *et al.*, 1998).

To further support the basolateral-like nature of the myelin sheet, we next investigated the effect of substituting a tyrosine residue for cysteine at position 543 in the the apical marker HA. In polarized epithelial cells, it has been demonstrated that this substitution causes internalization of the protein and switches sorting from the apical to the basolateral membrane surface (Brewer and Roth, 1991; Lazarovits and Roth, 1988). In figure 1D and 1E it is shown that whereas wt HA is particularly present in vesicle structures (as reflected by its punctate appearance) in the cell body and primary processes (cf. fig. 1D vs.1B), the mutant protein HAY+, next to a localization in the cell body, was also clearly discernable in the processes and myelin sheet (cf. fig. 1E vs. fig.1B). Importantly, the total expression levels of wt and mutant viral proteins were very similar (data not shown). These data thus indicated that substitution of amino acid residues, known to be critical to proper apical and basolateral sorting of proteins in polarized epithelial cells, also causes an analogous missorting in OLGs. The results thus reflect a similarity in sorting signals operating in both cell types and moreover, support the apical-like and basolateral-like features of cell body plasma membrane and myelin sheet, respectively.

Given that both viral proteins are typical membrane-localized proteins, we next considered the possibility that the mutations may have caused a change in their lateral distribution in the plane of the bilayer, their subsequent partitioning into different membrane microdomains possibly contributing to their sorting into different transport vesicles.

Replacement of cysteine at position 543 by a tyrosine causes HA to become TX-100 soluble in mature oligodendrocytes

In polarized epithelial cells HA associates with detergent resistant microdomains ('rafts', Scheiffele *et al.*, 1997; de Vries *et al.*, 1998). Importantly, distinct amino acid residues in the HA transmembrane domain are important for this association, as sequence substitutions in this domain ablate its association with rafts (Lin *et al.*, 1997). Previously, we demonstrated (de Vries *et al.*, 1998) that in OLGs, wt HA is recovered in a TX-100 insoluble fraction, a feature that is often associated with apical targeting and trafficking, whereas

VSV G is recovered in a TX-100-soluble fraction. To determine whether differences in sorting of the wt versus mutant proteins, as reported above, could (in part) have relied on alterations in detergent solubility, presumably reflecting a change in their lateral membrane distribution, TX-100 extractions were carried out at 4 °C of cells, expressing wt or mutant forms of VSV G and HA.

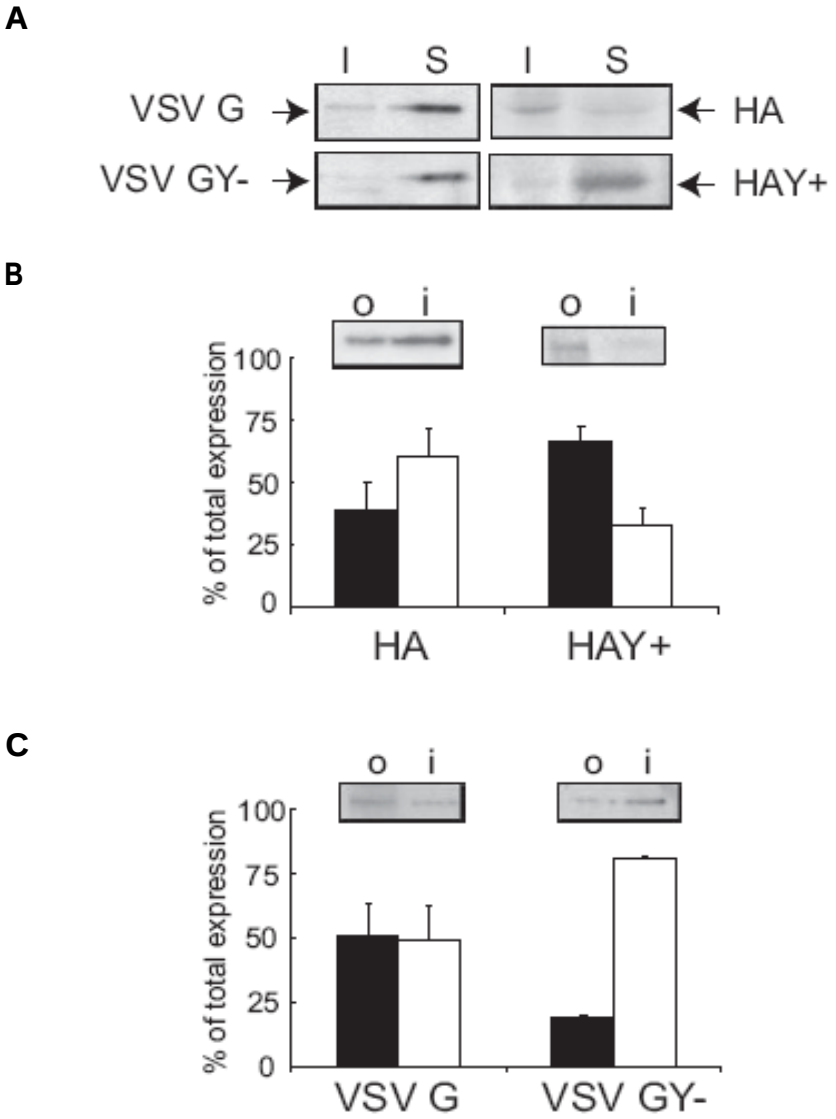

Figure 2: (A) Immunoblots of TX-100-soluble and -insoluble fractions of wild-type and mutant forms of VSV G and HA in primary mature OLGs. After TX-100 extraction at 4°C and centrifugation, insoluble (pellets) and soluble (supernatants) fractions were analyzed by Western blot for the distribution of the wild-type and mutant forms of HA and VSV G. Soluble and insoluble fractions are indicated by 'S' and 'I', respectively. Representative blots are shown of three independent experiments. Note that wt HA is mainly TX-100 insoluble, whereas mutant HAY$^+$ is TX-100 soluble and that VSV GY$^-$ remained detergent soluble. (B and C) OLG progenitors were retrovirally infected with (B) HA or HAY$^+$ and (C) VSV G or VSV GY$^-$ and surface biotinylated as described in Materials and Methods. The biotinylated (outside, o) and non-biotinylated (inside, i) protein fractions were analyzed by Western blot and quantified (bars underneath the blots), the white bar reflecting the inside fraction and the dark bar representing the biotinylated (surface exposed outside) protein fraction. Representative blots are shown. Data represent means ± SE of three independent experiments.

As shown in figure 2A, both VSV G and VSV GY$^-$ almost exclusively partitioned in the detergent soluble (S) fractions, indicating that the replacement of tyrosine at position 501 by a serine had not altered this distribution. Interestingly, whereas wt HA localizes to a major extent in the TX-100 insoluble fraction (I), HAY$^+$ primarily localized in the supernatant, indicating that a mutation at position 543 in HA eliminated its association with TX-100 insoluble microdomains (fig. 2A), thereby likely enabling transport to the myelin sheet.

HAY$^+$ and VSV GY$^-$ are not localized in the plasma membrane of mature oligodendrocytes

The results described above revealed that VSV GY$^-$ was mislocalized, prominently accumulating in the cell body, whereas introduction of a tyrosine in HA caused the protein to be transported (in part) to the myelin sheet. To determine whether the mutant proteins still resided at the membrane surface of either plasma membrane (cell body) or myelin-like membranes or that missorting also affected their (intra)cellular localization, OLGs were surface biotinylated following expression of wt and mutant forms of HA and VSV G. In figure 2B it is shown that the surface labeling of HAY$^+$ (o, black bar; right panel) is increased in comparison to the surface labeling of HA (o, black bar, left panel). Thus, nearly 75 % of the HAY$^+$ was accessible for biotinylation at conditions where only 35 % of HA was exposed at the cells surface. These data are consistent with the fluorescence localization data in figure 1, supporting the notion that upon missorting of HAY$^+$, the myelin sheet provides a larger surface area for membrane surface exposure than the cell body plasma membrane, which is essentially the target site of wt HA. By contrast, and consistent with an apparent strong diminishment of VSV GY$^-$ transport to the sheet (cf. fig. 1), in OLGs expressing the mutant protein only 20 % of the total protein fraction is expressed on its surface, while approx. 60 % of wt VSV G is surface-localized (fig. 2C). Hence, the cellular distribution of the proteins is likely not influenced by an altered surface expression, but rather by differences in protein distribution over the total surface area.

Having thus identified a remarkable similarity in (at least some) sorting signals operating in membrane transport of VSV G and HA in both polarized epithelial cells and OLGs, implying basolateral-like sorting features operating in transport to the myelin sheet, we next investigated some regulatory aspects of this pathway by examining the role of protein kinase C (PKC), previously shown to carefully regulate polarized membrane transport (Zegers and Hoekstra, 1997; Baron *et al.*, 1999; Tyteca *et al.*, 2005).

Trafficking to the myelin sheet is inhibited upon activation of PKC

In OLG progenitors, PKC activation by phorbol ester (PMA) causes a redistribution of actin filaments with a concomitant perturbation of VSV G transport from the TGN to the plasma membrane (Baron *et al.*, 1999). As shown in figure 3B (compared to 3A), in mature OLGs, PMA-induced activation of PKC caused a significant decrease in VSV G transport to the myelin sheet. The activation of PKC resulted in a punctate appearance of the VSV G protein within the processes (see arrows). Thus, these data demonstrate, and in essence are consistent with previous data obtained in OLG progenitors (Baron *et al.*, 1999), that PKC activation negatively regulates myelin sheet-directed transport, as characterized by transport of the basolateral marker VSV G. To investigate whether modulation of VSV G transport into the sheet reflected that of myelin-specific proteins as well, the effect of PKC activation on some resident myelin protein transport was monitored similarly. As shown in figure 3C in untreated cells proteolipid protein (PLP), next to a pool in the cell body, also prominently localizes to the myelin sheet, whereas treatment with PMA resulted in an effective inhibition of transport into the sheet (fig. 3D). Thus, like in the case of VSV G, a major part of PLP was largely retained in the cell body, its distribution within the processes showing a similar punctate distribution as observed for the viral protein VSV G (see arrows). Quantitative support for the pronounced impediment of PLP and the subsequent diminishment in the protein's surface localizaton was obtained by determining the relative overall membrane surface expression by means of surface biotinylation, after activation of PKC. These data are presented in figure 4 and demonstrate that upon activation of PKC, an enhanced fraction of PLP, from approx. 85 % at control conditions increasing to 99 % upon activation, is no longer localized at the cell surface. A likely explanantion for this observation is that transport vesicles, observed to accumulate in the processes (fig. 3D, arrows) are no longer able to dock, thereby precluding PLP insertion into the myelin membrane. The PKC inhibitor BIM counteracted the effect of surface transport, underscoring the specific involvement of PKC in modulating PLP transport to myelin-like membranes (fig. 4). Hence, these findings demonstrate that transport of a typical myelin protein like PLP, being an essential part of myelin biogenesis, is negatively regulated by PKC activation, as observed for VSV G marker protein. Another important myelin protein, myelin basic protein (MBP), is exceptional in that it is not transported to the myelin sheet as a protein.

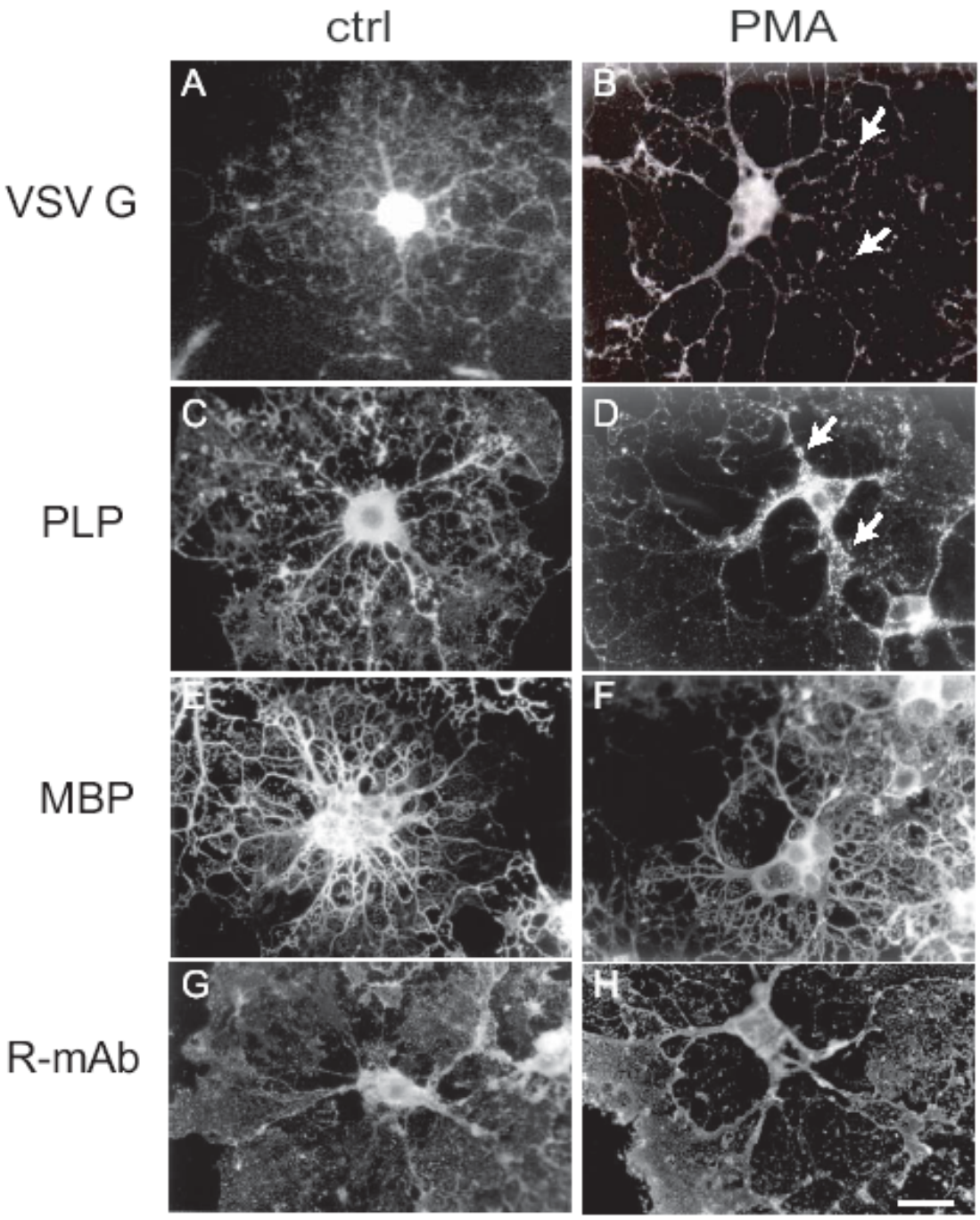

Figure 3: Effect of PMA-stimulated activation of PKC on transport of VSV G and resident myelin proteins in primary oligodendrocytes. In A, C, E, and G the localization of VSV G (A), PLP (C), MBP (E), and R-mAb (anti-GalCer/sulfatide, G) is shown in primary mature OLGs (ctrl) by immunofluorescence, using appropriate antibodies (see Materials and Methods). In B, D, F, and H the effect of prior treatment (24 hrs) of the cells with 100 nM PMA on protein distribution (same order as above) is shown. To express VSV G, primary mature OLGs were infected with VSV (A, B) as described in Materials and Methods. Representative cells out of three independent experiments are shown. Scale bar is 20 µm. Note that PMA-induced activation of PKC caused a punctate appearance of VSV G (B) within the cells (arrows). Upon PKC activation, PLP sheet labelling (D) is conspicuously absent and a similar punctuate appearance of fluorescence is present (arrows).

Rather, its messenger is transported into the sheet in a microtuble-dependent manner, where the protein is subsequently synthesized locally (Barbarese *et al.*, 1995; Boccaccio and Colman, 1995). Therefore, it is likely that its trafficking may be regulated differently from that of PLP. Indeed, as shown in figure 3E and F, the appearance of MBP, as opposed to that of PLP, is not affected by PKC activation. Interestingly, however, neither transport or localization of CNP was significantly affected upon PKC activation (not shown), CNP representing a myelin-specific protein that like MBP associates with myelin membranes, while its transport occurs by a non-vesicular transport mechanism.

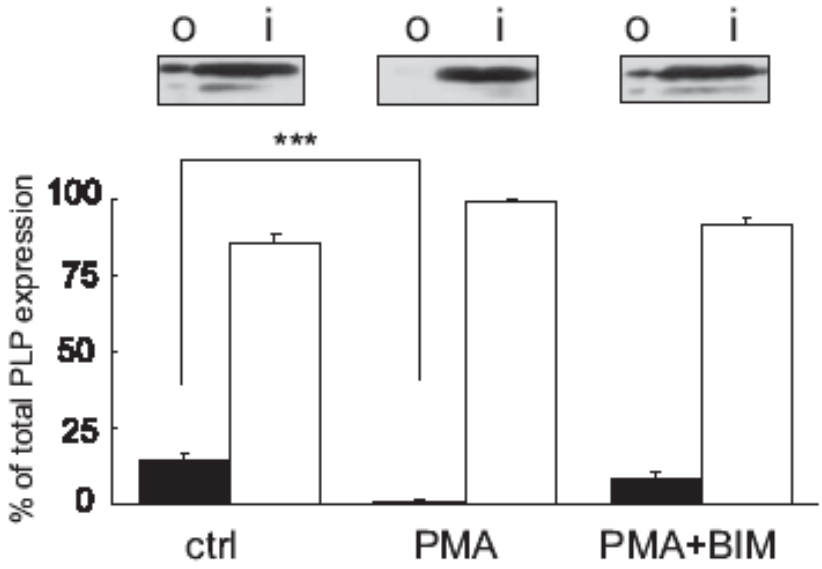

Figure 4: PKC activation inhibits the surface appearance of PLP. Primary OLG progenitors were differentiated for 10 days, and were untreated, exposed to PMA or exposed to PMA and BIM, followed by surface biotinylation to determine the surface-associated pool of the protein, as described in the Materials and Methods. In the upper panel the Western blot of the biotinylated fraction (outside, o) and the non-biotinylated fraction (inside, i) are shown. Note that on some of the blots a lower band is appearing, presumably DM20, which is an alterative spliced form of the plp-gene. The PLP-bands were quantified and a graphical representation of these data is shown underneath the blots, black bars representing the surface fraction and the white bar the fraction within the cells, i.e., not accessible to biotinylation. Representative blots are shown. Data represent means of three independent experiments. *** $p<0.001$.

In OLG progenitors, PKC activation inhibits morphological differentiation (Baron *et al.*, 1999; Šišková *et al.*, 2006), whereas long-term exposure at later differentiation stages suggests that PKC activation induces process outgrowth and myelination by mature OLGs, i.e., a more complex network (reviewed by Stariha and Kim, 2001). As shown in figure 3 (MBP and R-mAb), the morphological consequences of a relatively short-term PMA treatment (24 hrs) are minimal if apparent at all, when compared to untreated cells.

Indeed, also in cells stained with the R-mAb (anti-GalCer/sulfatide) the integrity of the sheet is seemingly maintained following PMA exposure (fig. 3G and 3H). Furthermore, the microtubule system is not significantly affected (data not shown), whereas differences in actin cytoskeleton restructuring are less compelling than in OLG progenitors (Baron *et al.*, 1999, Šišková *et al.*, 2006). We therefore exclude that effects on PLP transport are related to an indirect effect of PKC activation via an overall change in morphology.

Discussion

In the present study, we have further investigated the polarized nature of the cell body plasma membrane versus myelin sheet in oligodendrocytes. By employing viral marker proteins, i.e., hemagglutin HA and VSV G, which specifically target to apical and basolateral membrane domains in epithelial cells, respectively, we demonstrate that the same sorting signals as in epithelial cells are operating in OLGs in directing membrane domain-specific targeting of these proteins. Thus, transport to the myelin sheet is driven by a basolateral-like signal and vesicular trafficking is negatively regulated by PKC. Removing a tyrosine at position 501 in the cytoplasmic tail of the basolateral marker VSV G seriously impeded transport of the protein to the sheet, resulting in its apparent intracellular accumulation in the cell body. In case of HA, the Cys/Tyr mutation at position 543 caused a lateral redistribution of the protein, as suggested by a shift from a TX-100 insoluble to a TX-100 soluble membrane fraction, and its concomitant appearance in the myelin sheet instead of the cell body plasma membrane, the latter being seen for wt HA. Possibly, this difference in lateral membrane distribution underlies a difference in sorting based upon recruitment into distinct membrane transport vesicles, (co-)determining the eventual destination of the protein. In this context it is of interest to note that although the sheet is enriched in microdomain-stabilizing glycosphingolipids, displaying detergent resistance, the majority of the mutated HA (HAY^+) is detergent soluble, as opposed to the largely insoluble properties seen for the wt HA, which localizes in particular at the cell body plasma membrane. Importantly, the shift in membrane surface expression from body to sheet (HAY^+) or sheet to body ($VSV\ GY^-$) is quantitatively supported by biotinylation experiments, indicating that 'missorting' is not likely related to an impediment in vesicular transport to and/or inhibition of vesicle docking at the target membrane, as the appearance of the relative protein fractions at plasma membrane and sheet are consistent with differences in sorting/targeting direction of the mutant versus wt. In passing,

it should be noted that the net protein fraction actually expressed at the cell surface at a given time (and detectable by biotinylation; fig. 2) will depend on the effectiveness of target membrane-directed transport (following its biosynthesis) and the dynamics of the acceptor membrane (endocytosis and recycling), implying that an exclusive presence of HA or VSV G at the membrane surface is not realistic (c.f. fig. 1). Interestingly, impediment of transport and docking may underlie the mechanism by which PKC activation regulates sheet-directed trafficking (fig. 3). More intriguingly however, while transport of the basolateral marker VSV G and the resident protein PLP is impeded upon PKC activation, in part at the level of vesicle docking (cf. fig. 3B and D), these studies also revealed that sheet-directed transport pathways in parallel exist that operate independent of PKC, as observed for transport of CNP and MBP (mRNA), both of which were relatively unaffected upon PKC activation (fig. 3E and F). This distinction can be presumably attributed to the fact that whereas transport of the latter occurs via a non-vesicular mechanism (Gielen *et al.*, 2006, and references therein), transport of both VSV G and PLP, both representing integral membrane proteins, is vesicle mediated.

In previous work it was demonstrated that PKC activation by the phorbol ester PMA in OLG progenitors causes a perturbation of membrane-directed transport of VSV G (Baron *et al.*, 1999), an effect that was related to phosphorylation of MARCKS, a membrane-bound protein that is closely involved in maintaining the structural integrity of the actin cytoskeleton. Moreover, the physiological significance of this finding was recently demonstrated by showing that fibronectin inhibits myelin sheet directed trafficking via a similar PKC-dependent mechanism (Šišková *et al.*, 2006). The observed PKC-dependent mechanism of regulating sheet directed trafficking makes it thus likely that this basolateral-like transport pathway in OLGs depends on cytoskeletal elements. Indeed, cytoskeletal filaments are known to facilitate vesicular transport (Zegers and Hoekstra, 1998; Jacob *et al.*, 2003), and rearrangement of the actin cytoskeleton is thought to play an important role in the establishment and maintenance of cell polarity (Drubin and Nelson; 1996; Zegers and Hoekstra, 1997).

The present data further emphasize the unique polarity properties of OLGs. Clearly, in OLGs, sorting of VSV G to the sheet occurred via a tyrosine-dependent mechanism, also operating in basolateral sorting in MDCK cells, thus further highlighting the basolateral-like features of the sheet. Inclusion of a tyrosine signal in HA (HAY^+) similarly rerouted the protein to the sheet, in stead of the plasma membrane, with a concomitant loss of its localization

in a detergent resistant microdomain. In terms of its primary sequence, the created HA C543Y basolateral sorting signal resembles that identified in the VSV G (Thomas and Roth, 1994). It is then tempting to suggest that as a result the HA mutant might interact selectively with the same recognition molecules (AP molecules; cf. Gravotta *et a*l., 2007) for sorting, as those involved in targeting of native VSV G, thereby causing the apical-like protein HA to be targeted to the (basolateral-like) myelin sheet.

Of physiological relevance is the issue whether this tyrosine signal is also operating in sorting and transport of myelin specific proteins. The myelin-associated glycoprotein (MAG) is expressed as two isoforms, designated as the large isoform (L-MAG) and the small isoform (S-MAG) (Frail and Braun, 1985; Minuk and Braun, 1996; Erb *et al.*, 2006). L-MAG, containing an invariable basolateral sorting signal, is sorted to the basolateral membrane in MDCK cells, i.e., in a mechanistic sense reminiscent of the myelin sheet, whereas S-MAG rather depends on extrinsic factors, localizing to both the apical and basolateral membrane in MDCK cells (Minuk and Braun, 1996). Interestingly, L-MAG contains a crucial tyrosine residue (Tyrosine-620) in its D8 domain (the C-terminal domain specific to L-MAG). Moreover, both isoforms of MAG contain a sequence resembling a clathrin-coated pit internalization signal, including a tyrosine, which is crucial for basolateral sorting (Matter and Mellman, 1994). Of further interest, a dual tyrosine-leucine motif in myelin protein P_0 has been identified, which mediates basolateral targeting in MDCK cells (Kidd *et al.*, 2006). Finally, PLP contains a dileucine motif which localizes at the N-terminal region, immediately next to the palmitoylation sites, which were reported to be imperative for proper transport of PLP to the myelin sheet (Pham-Dinh *et al.*, 1991; Schneider *et al.*, 2005). Clearly, these examples warrant further investigations in the role of 'typical' basolateral and apical sorting signals in myelin protein transport and myelin assembly.

In summary, in the present work sorting signals have been identified for targeting membrane trafficking into the myelin sheet. In conjunction with specific signalling, vesicular trafficking into this pathway is regulated by PKC. However, trafficking of several myelin-specific resident proteins, which do not rely on vesicle-mediated transport including MBP (mRNA) and CNP, appears independent of PKC-dependent regulation. Accordingly a carefully coordinated expression and transport of individual proteins in myelin biogenesis and remyelination is required, desirable in case of disease-induced demyelination. A detailed understanding of these pathways may provide tools for exogenous modulation of these processes at disease conditions, which thus warrants further investigation.

Acknowledgments

We greatfully acknowledge the ffrench-Constant Lab (Cambridge, UK), especially Joao B. Relvas, for expert help in applying the retroviral expression system in oligodendrocytes. This work was supported by grants from the Dutch MS Research Foundation 'Stichting MS Research' (BK, WB) and the Foundation 'Jan Kornelis de Cock'.